ISSN 1070-4272, Russian Journal of Applied Chemistry, 2009, Vol. 82, No. 3, pp. 378–386. © Pleiades Publishing, Ltd., 2009.
Original Russian Text © A.V. Kuzema, A.A. Malygin, M.M. Ermilova, N.V. Orekhova, N.L. Basov, G.F. Tereshchenko, 2009, published in Zhurnal Prikladnoi Khimii, 2009, Vol. 82, No. 3, pp. 386–394.

PHYSICOCHEMICAL STUDIES OF SYSTEMS AND PROCESSES

Structural, Chemical, and Dynamic Characteristics of Ceramic Membranes Modified with Self-organized Supramolecular Silicon Oxide Systems

A. V. Kuzema, A. A. Malygin, M. M. Ermilova, N. V. Orekhova, N. L. Basov, and G. F. Tereshchenko

St. Petersburg State Technological University, St. Petersburg, Russia

Topchiev Institute of Petrochemical Synthesis, Russian Academy of Sciences, Moscow, Russia

Received January 14, 2009

Abstract—The changes in structural characteristics, chemical composition, and gas permeability of the modified ceramic asymmetric tubular membranes were studied. The membranes were tested in permeability and selectivity of two gaseous mixtures (H/He and H/Ar). The structure of the modified coating was examined by X-ray powder diffraction and by transmission and scanning electron microscopies.

DOI: 10.1134/S1070427209030070

Ceramic membranes (CMs) have found growing application in a variety of processes such as catalysis, sorption, separation, and filtration [1–7]. The important advantage of CMs is their thermal and chemical stability at relatively low cost, simplicity of recovery at enhanced temperatures, and high efficiency.

At the same time, owing to the specific features of the synthesis, CMs have low specific surface area (in comparison, for example, with microporous zeolite membranes) and are characterized by the nonuniform size distribution of transporting pores.

The various modification methods of pore filling (sol-gel procedure, chemical vapor deposition, and molecular layering [2, 6, 8, 10]) are used to optimize the CM structure.

Another method of the modification of wide pore ceramic membranes is synthesis on their surface or inside their pore volume of zeolite films [1,2]. However, such structures are brittle and labor-consuming in preparation.

Coating of CM surface with mesoporous thin silica films is also the promising modification method. The film synthesis is based on the procedures of structural self-organization (SSO), which is a spontaneous organization of materials via non-covalent interactions (hydrogen bonds, van der Waals and electrostatic forces, etc. [13]) occurring without application of external forces. In this case, it is possible to realize the narrow pore-size distribution and control it by varying the synthesis conditions.

Silicon-containing structures have high chemical and thermal stability, can be easily formed by the above method, and their films have high adhesion to the surface of oxide ceramics. Therefore, the goal of this study was to synthesize the silica films with desired properties on the surface of alumina-based CM and to study the effect exerted by them on the structure and permeability of the porous support.

EXPERIMENTAL

Planar mesoporous thin films were deposited onto the standard 50×25-mm slides of 2-mm thickness. As initial CMs were used asymmetric porous ceramic tubes made of α-Al_2O_3 (outer diameter from 5.5 to 7.3 mm, wall thickness 1.1–1.3 mm) with a sol-gel layer (thickness about 100 μm, mean pore diameter 50 nm) on their outer surface.

Silica films were synthesized from the solutions of the reagents to obtain mesostructural systems of three pore sizes (2, 3–4, and 5–6 nm).

Their structure was confirmed by the X-ray small-angle scattering and transmission electron microscopy (TEM) analyses of the model mesoporous thin films (MTF) on glass. All three mother solutions were prepared in two stages. In the first stage, a pre-hydrolyzed solution of tetraethoxyorthosilane (TEOS, Acros) was prepared by recirculation of a mixture of TEOS, ethanol (chemically pure, additionally distilled), hydrochloric acid (chemically pure), and distilled water (component molal ratio 1:3:5:103:1) through the fluidized bed for 60 min. Then, the acidified water-alcohol solutions of cross-linking polymers were prepared. To synthesize films with 2-, 3-, and 6-nm pores, we used cetyltrimethylammonium bromide (Merck), Brij 58 (Aldrich), and Pluronic F-127, respectively. The reagent ratio provided the component ratio TEOS:EtOH:HCl:H_2O: PAV = 1:20:0.004:5:0.01 in the final solution. All reagents, with the exception of hydrochloric acid, were used as purchased.

The modifying coatings were deposited by immersing the substrate into the solution and then by withdrawing it at a rate of about 1 cm min^{-1}. The composite obtained was dried at 150°C for 2 h and extracted in a 50 wt % sulfuric acid for 8 h at a boiling temperature of the mixture [14]. Then, the composite was washed with distilled water to neutral pH and dried at 150°C for 2 h.

The efficiency of deposition and the properties of a modifying silica film were evaluated for the case when film is formed on the outer surface of the support and for the case when it is formed in its intrapore volume. In the first case, CM samples were impregnated with *m*-xylene [pure grade, TU (Technical Specifications) 6-09-2438-82], then silica film was deposited by the above method, and after that, *m*-xylene was removed from intrapore volume. In the second case, CM samples were fully impregnated with a mother solution (fully impregnated samples), as described above, which would cause pore closing to occur not only on the CM outer and inner surfaces, but in its bulk too. Some samples were also synthesized by depositing a modifying coating two times.

The surface of the modified samples was studied on a CamScan MX2500 Scanning electron microscope equipped with a Link Pentaphet X-ray microanalyzer and Oxford Instrument Si/Li detector (area 10 mm^2, SATW window, resolution 133 eV, MnK_α radiation, accelerating voltage 20 kV). The probe current, as measured on a Faraday cylinder, was 1 nA and the working distance was 35 mm. Certified synthetic compounds and natural minerals were used as reference. As evaporation material served gold. The spectrum accumulation time (not including loading of an analog-to-digital converter) was 70 s.

Transmission electron microscopy was performed on a Philips CM 300 UT instrument (accelerating voltage 300 kV).

The X-ray powder analysis was done on a Bruker AXS Advance diffractometer (CuK_α line was used for mesoporous thin films on glass and CoK_α line, for modified CMs) at room temperature. Note, to evaluate the degree of pore filling with amorphous silicon dioxide, both tubular supports and powders obtained by their grinding were examined by X-ray analysis.

The small-angle X-ray scattering analysis needs samples with as much as possible planar surface providing accurate measurement of the incidence angle. For glassy supports, which were used to test the deposition technology of mesostructured films, no special treatment of the composite is required, whereas for tubular ceramic membranes with as high as 10-mm pore diameter, obtaining of large planar surface sufficient for the analysis meets certain difficulties. To do this, samples must be ground into powder or divided into segments and then put together into planar layer. The first procedure is less preferable, because in this case, data on the layer-by-layer assembly of the sample are lost. In the case of the second procedure, data on the surface layer structure may be obtained, but the error in determining the incidence angle for inhomogeneous mosaic structure is higher.

The dynamic characteristics of the initial and modified CM samples were evaluated by their gas permeability at room temperature. To do this, we used a diffusion cell schematically presented in Fig. 1. The pressure in the input chamber of the cell (inside the tube) was varied. A flow of the gas (helium, argon, or hydrogen) was delivered into the input chamber and the gas flow in the outlet of the output chamber was measured. The pressure in the input chamber was measured with a manometer 1. The output chamber was maintained at atmospheric pressure.

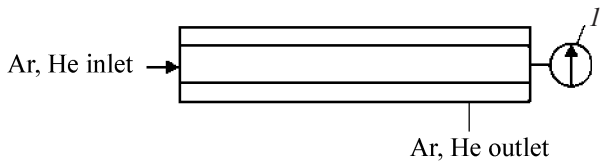

Fig. 1. Scheme of a diffusion cell for measuring gas permeability of asymmetric tubes. (*1*) Manometer.

Asymmetric molecules, which by nature tend to organize ordered supramolecular structures, are commonly used in SSO processes (as it is done in preparation of Langmuir-Blodgett films). To such molecules belongs PAV or polymers containing hydrophilic and hydrophobic moieties in the same molecule. In this study, hexadecyltrimethylammonium bromide CTABr ($C_{19}H_{42}BrN$, M = 346.46 g mol^{-1}) was used as ionic PAV. PAV Brij 58 [$C_{16}H_{33}(OCH_2CH_2)_nOH$, $n \sim 10$, $M_n \sim 683$ g mol^{-1}] served as nonionic polymer and Pluronic F-127 ([$H(OC_2H_4)_x(OC_3H_6)_y(OC_2H_4)_z$], $n \sim 14$, $M_n \sim 600$ g mol^{-1}), as block copolymer.

At PAV concentrations in the solution exceeding a critical value, the PAV molecules form spherical or cylindrical micelles [15] as consequence of orientation of the hydrophilic molecular moiety along the solvent molecules. In this case, the hydrophobic moiety is inaccessible to solvent molecules inside the micelle. At further increase of the PAV concentration, micelles organize hexagonal, cubic, or layered aggregates, which interact with the dissolved silicate particles to form an ordered organosilicate composite, which, after removal of organic substituent, is transformed into a mesoporous material with the ordered distribution of pores by size and structure [15].

An alternative method, evaporation-induced self-organization (EISO), was used in this study in the course of deposition of a mesostructured thin film (MTF). Beginning from homogeneous very dilute weakly acid solutions of the water-ethanol-PAV-silicate system, in which PAV concentration is considerably less than a critical value, selective evaporation of ethanol from the solution deposited onto the support in form of a thin film concentrates the solution with cosolvent (water) and nonvolatile silicate particles. The increasing PAV concentration initiates self-organization of SiO_2 micelles at the liquid-gas and liquid-solid interface and their further transformation into a liquid-crystalline phase. The SiO_2–PAV mesostructures, formed in a solution below critical concentration, serve as centers of growth and orientation of newly forming mesophase, which leads to the fast (on the order of tens of seconds) formation of the oriented structures near both interfaces. Large liquid-crystalline domains grow from the interfaces inside the layer being structured. After the solidification of the film is complete (solidification line), a composite consisting of disordered micelles (spaghetti structure) is formed between the more ordered layers [15]. A further maturing of the structure, the exposure of composite to acidic or alkaline catalyst, or its thermal treatment lead to polymerization of a silicon dioxide skeleton, and, consequently, to the fixation of the desired structure.

Results obtained in studying the structure of the silicon dioxide films on planar glassy support are demonstrated in Figs. 2a, 3. Prior to coating deposition, glasses were exhaustively washed and then dried at 150°C. To make *the structure formation* complete, freshly deposited films were dried at 150°C for 2 h in air, extracted in 50% sulfuric acid, washed with deionized water, and then dried again. As a result, transparent colorless films with good adhesion to glass surface were obtained.

The results of the performed study show that products, which, according to the X-ray (Fig. 2a) and TEM analyses (Fig. 3), can be described as a set of ordered pores packed into the cubic or hexagonal two-dimensional structures, are formed depending on the chemical composition of the mother solution (i.e., on the type of cross-linking polymer). The cubic structure is characterized by pores about 2 and 4 nm in diameter and the hexagonal structure, by 6-nm pores.

The use of the above process for the direct deposition of mesostructured films onto wide pore tubular α-Al_2O_3 CM, contrary to the case of the deposition onto planar nonporous support, is impeded by the fact that the formation of a mesostructured material inside the wide pores of the support is suppressed [16-18]. To overcome the interfering effect of widely porous support (for example, α-Al_2O_3), the macropores were preliminarily filled with a material, which may be then removed from the support, with a thin mesostructured layer on the surface of a wide pore α-Al_2O_3 remaining [17, 19]. This procedure has been used to synthesize the hexagonal and cubic phases (of the type of MCM-48) on the surface of wide pore tubular support [17].

In this work, we studied the possibility of CM coating with a mesoporous film with the pore ordering

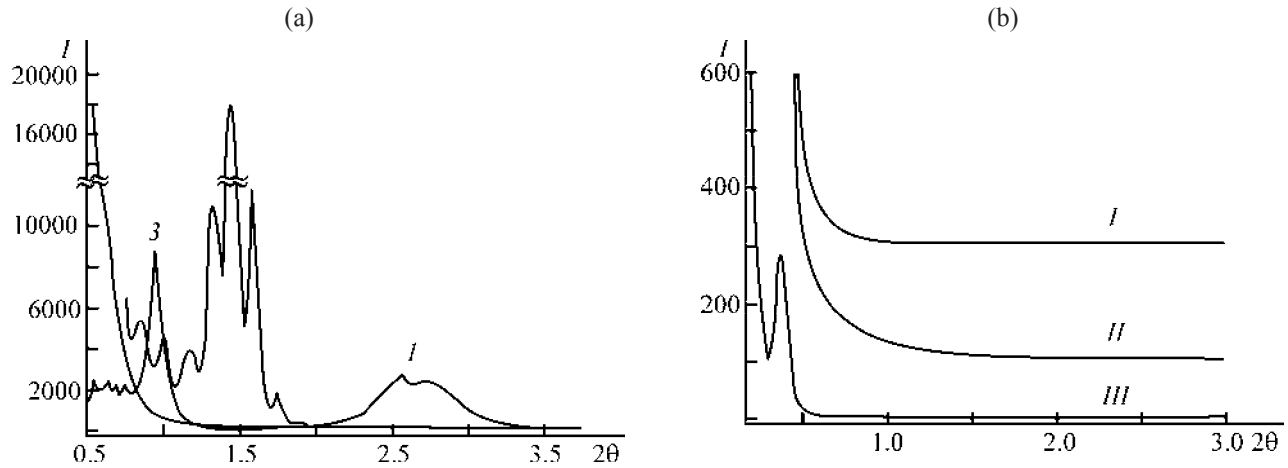

Fig. 2. Low-angle X-ray scattering on (a) mesostructured thin films on planar glassy support and (b) CM modified with mesoporous structures. (*I*) Intensity (pulse s^{-1}) and (2θ) Bragg angle (deg). (a) Pore size (nm): (*1*) 2, (*2*) 4, and (*3*) 6. (b) Membrane: (*I*) initial, (*II*) impregnated, and (*III*) coated.

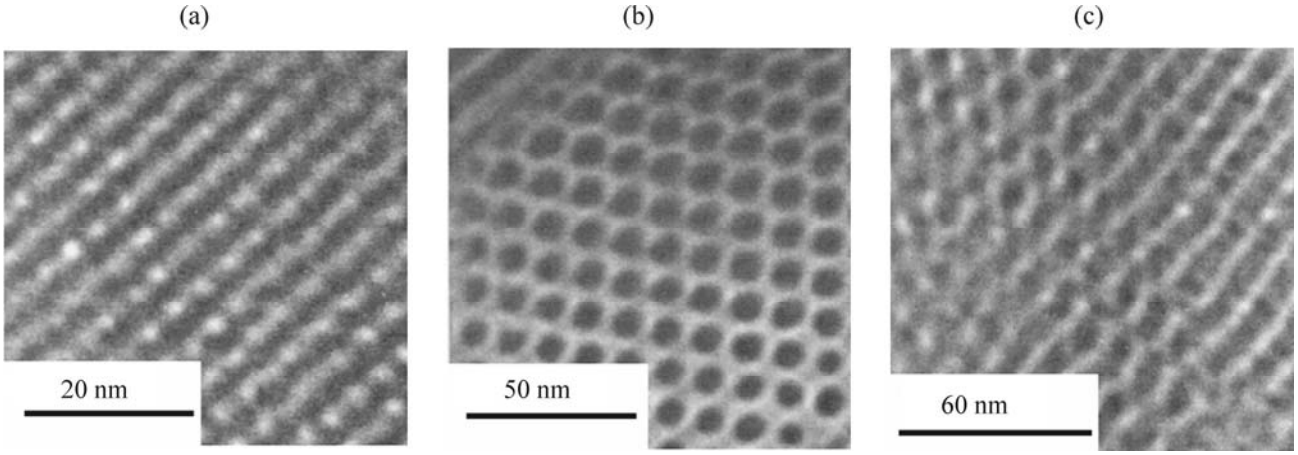

Fig. 3. Transmission electron micrograph of the silicate MTFs of three different pores sizes *d*. *d,* nm: (a) 2, (b) 4, and (c) 6.

and size other than those described in [17]. In synthesis of multilayer mesostructures we used a modified method [17] based on the Grosso et al. method [20, 21]. *m*-Xylene served as filler of CM micropores owing to its viscosity, which impeded its washout at the stage of the coating deposition, ensured its penetration into CM pores, and provided its removal at the stage of the intermediate heating of the support in the course of the synthesis. Some samples not modified by pore filling with *m*-xylene were impregnated with the mother solution for comparison (full impregnation).

The X-ray diffraction patterns of (*I*) non-modified CM, (*II*) fully impregnated CM, and (*III*) CM modified by pore filling with xylene and then coated with a mesoporous films are demonstrated in Fig. 2b. As follows from the results obtained, no ordering is present neither in the first, nor in the second case. In the case, when a modifying coating was deposited onto CM preliminarily filled with *m*-xylene, a reflection corresponding to the organized 30-nm structures is present. The size of periodic structures was calculated using the generally accepted procedure, i.e., by substituting the known parameters (Bragg angle 2θ and X-ray diffraction wavelength) into the Bragg diffraction equation $n\lambda = 2d\sin\theta$. The reflection peak is obtained in the diffraction pattern as a result of constructive interference of waves scattered from planes separated by the interplanar distance d. Because the measured structures were on the order of few and even tens nanometer size and the diffraction

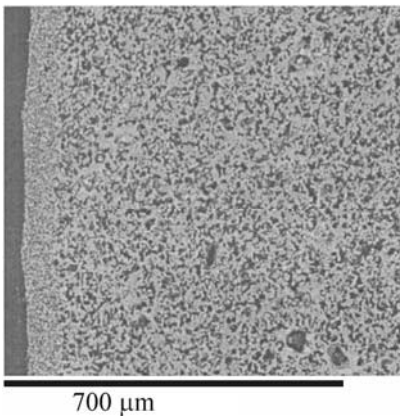

Fig. 4. Scanning electron micrograph of the section of the asymmetric tubular membrane.

wavelength was less than 2 Å, reflections should be at scattering angles on the order of 1 deg and lesser. To pass from periodic structures to pores, we used the additional, for example TEM, data on the pore wall thickness.

We used transmission electron microscopy to visualize pores and determine their local order. Prior to microscopic examination, samples were scrapped from the substrate and transferred onto a copper mesh. The local order was determined by the Fourier image analysis of a selected structural fragment. Such measurements gave 2, 4, and 6 nm for pore size and 1.5–2 nm for pore wall thickness. For a 4-nm pore sample, one of the layers of mesostructured coating of about 100-nm thickness is clearly revealed, in addition to pores. The Fourier analysis of the structures inside such layer gives the same values for the inverse sizes inside the layer (about 0.25 nm^{-1} for 4-nm pores) and the different value (about 0.3 nm^{-1}) for the direction normal to the layer. This is caused by compression of thin-film structures on heating, which preferentially occurs in the direction normal to the layer surface [15]. The results obtained confirm once again that "stripes" on the micrography are cross sections of layered structure of the film.

The modified CMs samples used in TEM analysis were cut with a diamond disc in the direction normal to the axis, immersed into epoxy resin, polished on a micrometer diamond paste, ultrasonicated in distilled water for 10 min to remove polishing material from CM pores, dried at room temperature, and coated with an electrically conducting gold layer.

In the study, the cross section of the asymmetric tubular CMs was visualized (see Fig. 4) and the degree of filling of alumina skeleton with amorphous SiO_2 was determined by the chemical analysis of a near-surface layer (see Fig. 5).

As seen from Fig. 4, CM is the asymmetric widely porous membrane of about 1.5-mm thickness coated with a near-surface layer of finer pores of about 100-μm thickness. Inside this finely porous layer (or on it outer surface), amorphous or mesostructured silica layer is preferentially formed, depending on deposition conditions.

Though by visual observation, the photomicrographs of the sections are indistinguishable for modified and non-modified membranes (see Fig. 5, inserts), their chemical composition determined at a step of 20 μm below the surface inside CM is different.

As seen, the silicon content decreases in the order: sample F, sample F2, and non-modified sample R1. Interestingly, the distribution of aluminum is opposite to that of carbon. Apparently, region poor in aluminum is occupied by a pore filled with epoxy resin, which is responsible for the carbon peak, and, on the contrary, in a region richer in aluminum, aluminum incorporates into the matrix wall, thus impeding penetration of epoxy resin through the material.

The distribution of Si and Al also shows that the silicon content is the largest at a depth from 20 to 240 μm from the surface of fully impregnated sample (Fig. 5b). Apart from this, the Al and Si contents in this sample are distributed in the opposite order. This result is likely to show that to a depth of 240 μm the silicon oxide structures are formed inside the pores rather than on the pore walls.

It seems somewhat unusual that the silicon content on the CM outer surface, modified by filling of the intrapore space with *m*-xylene and then coated with a structured film, is lesser than that on the outer surface of initial tube. This may be due to degradation and peeling off a part of silica film upon xylene removal. In addition, the thickness of a near-surface layer and, consequently, the silicon content in it may be so small that difference between modified and non-modified membranes can be well explained by contamination of the latter in the course of the sample preparation.

The effect of modification on the dynamic characteristics of CMs was evaluated by gas permeability and selectivity of non-condensed gases (hydrogen, helium, and argon). The measured value of the gas flow V through the CM, as reduced to the geometric surface of corresponding space between the tube, was accepted as

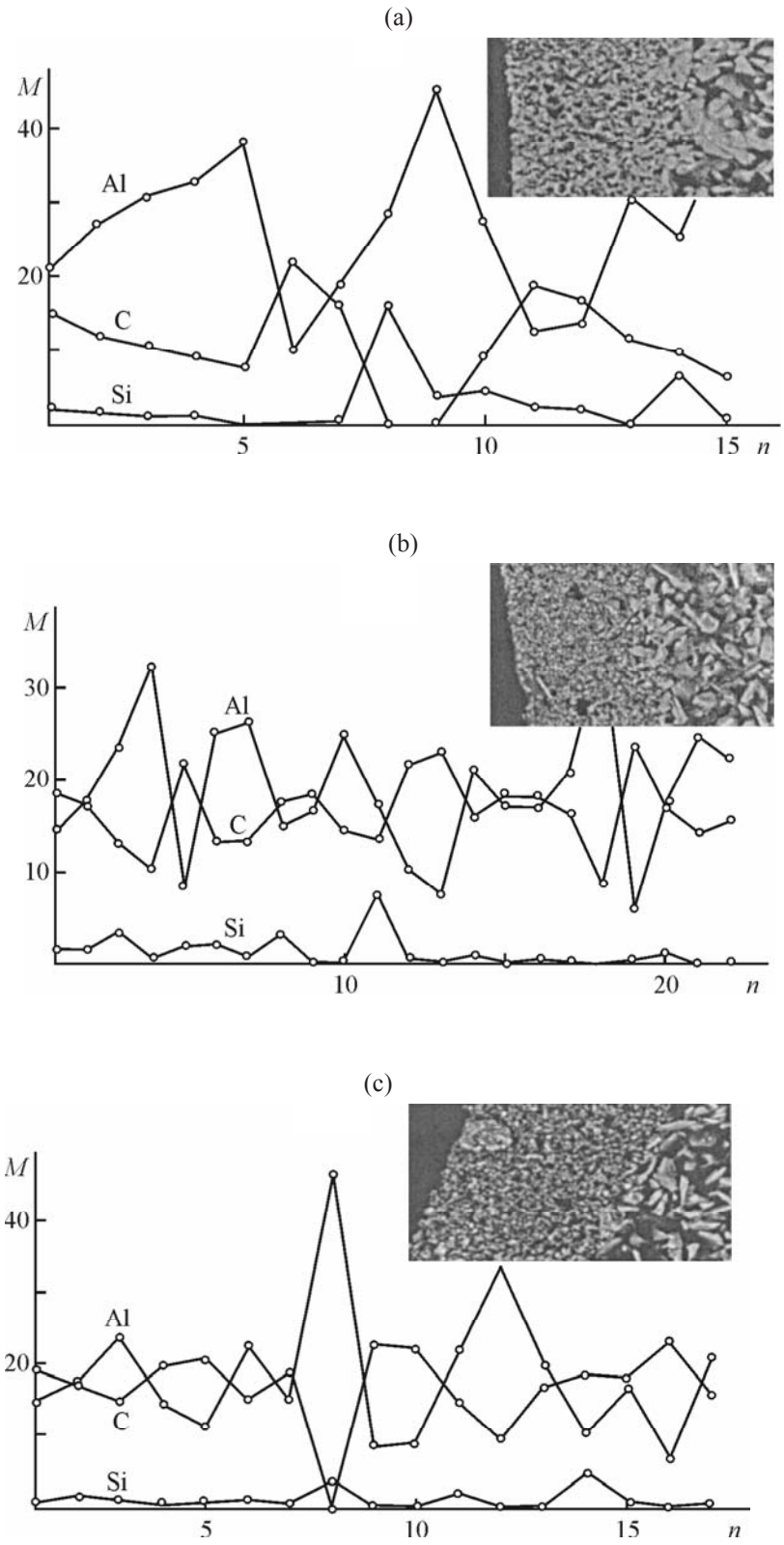

Fig. 5. The content *M* (wt %) of Si, C, and Al in the samples. (*n*) Number of measuring step (distance between steps 20 μm). CM: (a) initial (sample R1), (b) infiltrated (sample F), and (c) coated with SiO_2 film on the surface (sample F2). Inserts are microphotographs corresponding to regions under examination.

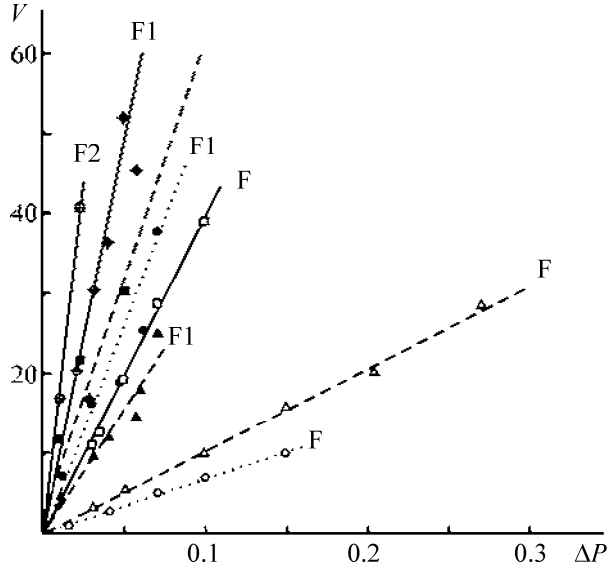

Fig. 6. Permeability V (ml min^{-1} cm^{-2}) of the F, F1, and F2 samples vs. pressure drop $\Delta P = P_1 - P_2$ (atm). Gas: hydrogen (solid), helium (dashed), and argon (dotted). Mark: Light (sample F), dark (sample F1), and crossed (sample F2). (Point) Experimental and (line) found by approximation. Equations for the obtained straight lines were determined by the linear regression method using the Origin 6 computer program.

a measure of gas permeability. The gas permeabilities were plotted as functions of the pressure difference (atm) between the input and output chambers.

The $V = f(\Delta P)$ graphs for tubes F are demonstrated in Fig. 6 as example. The equation parameters for the obtained straight lines were determined by processing of data by a linear regression method in the Origin 6 computer program.

The results of the measurement are given in Table 1, along with the calculated permeability coefficients B and corresponding correlation coefficients R^2. The separation factors F for this gas mixtures, as found from the relative hydrogen to helium (or argon) pressure P are also given for each tube.

The best selectivity of a hydrogen-argon mixture has tube F. The separation factor for this tube (4.5) exceeds that typical of Knudsen capillary flow. In a hydrogen-helium mixture, the separation factor for this tube is 3.9, i.e., also higher than for ideal Knudsen flow (3.16). In this case, the permeability coefficients of the studied mixtures appeared by a factor of 2–5 lower than those for non-modified tube R1. This may be due to the continuous pore filling of the fine pore layer of asymmetric CM by amorphous (not meso-structured) silicon oxide. This suggestion is also confirmed by the low-angle X-ray scattering analysis, which revealed no any ordered structure (Fig. 2b). No one of the remainder tubes reaches the theoretical values of the separation factors.

Table 1. Gas permeability characteristics of initial and modified ceramic asymmetric porous tubular membranes

Tube index	Tube characterization	Working surface area, cm^2	Permeability equation $V = B\Delta P + A$, ml cm^{-2} min^{-1}			$F_{H/He}$	$F_{H/Ar}$
			gas	B	R^2		
R1	Initial tube (large d)	4.4	H	1103.3	0.999	2.0	3.6
			He	541.4	0.99		
			Ar	310.3	0.994		
R2	Initial (small d)	2.8	H	1800.8	0.999	1.8	3.5
			He	1018.2	0.991		
			Ar	516.2	0.99		
F	Completely impregnated (small d)	3.5	H	397.4	0.998	3.9	6.0
			He	103.5	0.999		
			Ar	67.1	0.998		
F1	Completely impregnated (large d)	4	H	1006.5	0.9	1.8	3.3
			He	544.1	0.954		
			Ar	308	0.971		
F2	Coated with two a two-layer film (small d)	3.3	H	1760.2	0.999	1.8	2.9
			He	994.7	0.994		
			Ar	598.6	0.973		

Table 2. Selectivity characteristics of CMs in the course of step-wise modification by the mesoporous coatings of different pore diameters(~5 nm for samples 1, 1F and ~3 nm for samples 2, 1V)

Tube index	Tube characterization	Working surface area, cm^2	Permeability equation $V = B\Delta P + A$, ml cm^{-2} min^{-1}			$F_{H/He}$	$F_{H/Ar}$
			gas	B	R^2		
0	Initial, not coated	6.2	H He Ar	370.2 262.3 126.1	0.999 0.994 0.999	1.4	2.9
1	One-layer of coating	5.6	H He Ar	311.81 157.25 99.1	0.988 0.999 0.933	2.0	3.2
2	The same	5.1	H He Ar	249.0 172.2 75.83	0.989 0.999 0.997	1.4	3.3
1F	Repeated deposition onto sample no. 1	5.1	H He Ar	98.94 56.27 30.97	0.989 0.995 0.997	1.8	3.2
1B	Repeated deposition onto sample no. 2	5.8	H He Ar	317.0 186.0 91.3	0.997 0.998 0.999	1.7	3.5

Repeated deposition of layers onto the tubes yields controversial results. For one sample, there are virtually no changes, whereas for another one, the selectivity somewhat increases (Table 2).

For all the samples subjected to full impregnation without preliminary pore filling with xylene the selectivity values are close, irrespective of the chemical composition of the mother solution, i.e., on the type of a cross-linking polymer (Table 3). This shows that the silica structures formed inside the porous ceramic matrix are similar, and no meso-structures differing in the pore sizes are present.

CONCLUSIONS

(1) Ordered pores of 2, 4 and 6-nm size are found on planar glassy support, depending on the chemical composition of the mother solution.

(2) The ordered mesoporous structures are formed on the surface of wide pore ceramic membranes only after preliminary pore filling, which is in line with the latest studies in this area.

(3) The porous system of asymmetric ceramic membranes was modified. As a result, its permeability decreased and selectivity changed. The various values of the parameters were obtained, depending on treatment. The selectivity of the fully impregnated sample increased from 2 to 3.9 in the N/He mixture and from 3.6 to 6 in the H/Ar mixture. The selectivity of the sample coated with a thin mesostructured layer remained virtually unchanged (to within determination error) [(2 and 1.8) in the H/He mixture and 3.6–3.3 in the H/Ar mixture]. The lack of coating effect on the membrane parameters says that its thickness is insufficient for effective operation.

Table 3. Change in selectivity of the initial CMs after full impregnation with the solutions differing in the types of cross-linking polymers

Sample	Tube character-istics	Tube diameter d, mm	$F_{H/He}$	$F_{H/Ar}$
R1	Initial	7.3	2.0	3.6
F1	Wide pore (Pluronic F-127 polymer)	7	1.8	3.3
B1	Medium-pore (Brij 58 poly-mer)	7	1.6	2.8
C1	Fine pore (CTABr)	7	1.8	3.6

ACKNOWLEDGMENTS

The authors are deeply grateful to Dr. A. Antonov (*All-Russia Research Institute of Geology*, *Center of Isotopic Investigations, St. Petersburg, Russis*) for assistance in the scanning electron microscopy examination of modified ceramic membranes, Dr. G. Kokh (JLU-Giessen, Germany) for scanning electron microcopy analysis of mesoporous thin-film composites, Dr. M. Yagovkina (Ioffe Physicotechnical Institute, Russian Academy of Sciences, St. Petersburg, Russia) for the X-ray analysis of modified ceramic membranes, and Yu. Bykov (*All-Russia Research Institute of Geology*, *Center of Isotopic Investigations, St. Petersburg, Russia*), who helped in preparation of samples for scanning electron microscopy and assisted in assembling experimental set-up.

REFERENCES

1. Pan, M., Cooper, C., Lin, Y.S., and Meng, G.Y., *J. Membr. Sci*., 1999, vol. 158, no. 1, p. 235.
2. Xomeritakis, G., Han, J., and Lin Y.S., *J. Membr. Sci*., 1997, vol. 124, no. 1, p. 27.
3. George, S.M., Ott, A.W., Klaus, J.W., et al., *Appl. Surface Sci*., 1996, vol. 107, p. 128.
4. Kagramanov, G.G., and Nazarov, V.V., *Steklo. Keram*., 2001, no. 5, pp. 12, 39.
5. Aleksandrin, A.P., Alekseev, S.Yu., Egorshev, A.A., et al., Abstracts of Papers, *Vserossiiskaya nauchnaya konferentsiya "Membrany–2001"* (All-Russian Scientific Conf. "Membranes-2001"), Moscow, October 2–5, 2001, p. 134.
6. Kagramanov, G.G., Kholkin, P.V., and Lukashev, E.A., *Ogneupory. Tekh. Keram*., 2001, no. 5, p. 2.
7. Bashtan, S.Yu., Goncharuk, V.V., Chebotareva, R.D., and Linkov, V.M., *Elektrokhimiya*, 2001, vol. 37, no. 8, p. 912.
8. Kol'tsov, S.I., and Aleskovskii, V.B., *Zh. Fiz. Khim*., 1968, vol. 42, p. 1210.
9. Aleskovskii, V.B., *Zh. Prikl. Khim*., 1974, vol. 47, no. 10, p. 2145.
10. Malygin, A.A., *Khimya poverkhnosti i nanotekhnologiya vysokoorganizovannykh veshchestv* (Surface Chemistry and Nanotechnology of Highly-Organized Substances), Collection of Sci. Works, St.Petersburg.: St. Pet. Gos. Tekhn. Inst (Tekh. Univ.), 2007, p. 22.
11. Piera, E., Giroir-Fendler, A., Dalmon, J.A., et al., *J. Membr. Sci*., 1998, vol. 142, no. 1, p. 97.
12. Yawalkar, A.A., Pangarkar, V.G.,and Baron, G.V., *J. Membr. Sci*., 2001, vol. 182, nos. 1–2, p. 129.
13. van Water, L.G.A., and Maschmeyer, T., *Topics in Catal*., 2004, vol. 29, p. 67.
14. Wang, Y., Zibrowius, B., Yang, C.-M., et al., *Chem. Commun*., 2004, no. 1, p. 46.
15. Lu, Y., Ganguli, R., Brinker, C.J., et al., *Nature*, 1997, vol. 389(6649), p. 364.
16. Kouzema, A.V., Froba, M., Chen, L., et al., *Adv. Func. Mat.,* 2005, vol. 15, no. 1, p. 168.
17. Liu, C., Wang, J.,and Rong, Z., *J. Membr. Sci*., 2007, vol. 287, no. 1, p. 6.
18. Xomeritakis, G., Braunbarth, C.M., Smarsly, B., et al., *Micro. Meso. Mater*., 2003, vol. 66, no. 1, p. 91.
19. Kim, Y.S., and Yang, S.M., *Adv. Mater*., 2002, vol. 14, p. 1078.
20. Grosso, D., Cagnol, F., Soller-Illia, G., et al., *Adv. Funct. Mater*., 2004, vol. 14, no. 15, p. 309.
21. Klotz, M., Albouy, P.-A., Grosso, D., et al., *Chem. Mater*., 2000, vol. 12, no. 6, p. 1721.